IFSCC 2025 full paper (IFSCC2025-814)

Assessing Chemical Treatment-Induced Hair Damages and Conditioner Recovery Efficacy Utilizing Integrative Analytical Approaches Supported by Nuclear Magnetic Resonance (NMR) Spectroscopy

Minjoo Noh* [1], Quynh Thi Nguyen[2], Seyoung Yang[2], Jihui Jang[1], Jihyun Lee[1], Heemuk Oh[1], Sung Yun Hong[1], Seoyoon Lee[1], Chun Ho Park[1], Junbae Lee[1], Youngbok Lee[3]

[1]R&I Center, COSMAX, Seongnam-si, Republic of Korea
[2]Applied Chemistry, Hanyang University, Ansan, Republic of Korea

1. Introduction

Human hair plays an essential role in protecting the scalp and contributes significantly to personal appearance and identity. Hair is primarily composed of keratin, a fibrous protein that provides mechanical strength and elasticity through a well-organized hierarchical organization. It consists of the cuticle, cortex, and medulla, with the cuticle serving as the outermost protective layer [1,2]. Keratin also has two major types of secondary structure which are the α-helix and the β-sheet [3,4]. The mechanical and chemical stability of hair is enhanced by intermolecular interactions such as hydrogen bonds and disulfide bonds, particularly within the α-helix region of keratin [5]. Melanin pigments, including eumelanin and pheomelanin, account for about 1–3 wt.% of human hair alongside α-keratin [6]. These pigments not only determine hair color but also protect against UV radiation and bind selectively to heavy metals and toxins, aiding their removal from the body [7,8].

Recently, hair styling to achieve a desired hair aesthetic has become popular, and techniques such as perming, dyeing, and bleaching are used for this purpose. These procedures involve strong oxidizing or reducing agents, such as hydrogen peroxide and ammonium thioglycolate, which can alter the chemical composition and compromise the structural integrity of hair [9]. Bleaching, in particular, not only decolorizes melanin pigments but also oxidizes cysteine residues, leading to the cleavage of disulfide bonds and degradation of the keratin structure [10,11]. The cumulative effects of such treatments manifest as increased surface roughness, loss of moisture retention, decreased tensile strength, and higher porosity.

A variety of analytical techniques have been used to investigate the effects of cosmetic procedures on hair fibers, including Raman spectroscopy, X-ray diffraction, fluorescence spectroscopy, Fourier-transform infrared (FT-IR) spectroscopy, and solid-state nuclear magnetic resonance (NMR) spectroscopy [12-15]. Despite these advances, most previous studies have focused on limited aspects of damage and recovery, analyzing only surface morphology and primary structural changes. To elucidate the extent and underlying mechanisms of hair damage, it is essential to conduct precise analyses of melanin oxidation and structural changes in α-keratin following exposure to hair treatments. A multi-analytical approach that integrates various techniques is effective for this purpose. Notably, the restorative effects of post-treatment

products, such as conditioners containing active ingredients, have not yet been sufficiently characterized by advanced tools, highlighting the need for systematic investigation.
In this study, we employed analytical techniques including scanning electron microscopy (SEM), FT-IR spectroscopy, fluorescence spectroscopy, and solid-state ^{13}C NMR spectroscopy to investigate the effects of different chemical treatments on hair. The restorative conditioner formulation was applied to real damaged hair to determine its effectiveness using high-resolution magic angle spinning (HR-MAS) NMR spectroscopy. This approach enables us to visualize the surface damage caused by chemical treatments, detect molecular-level changes such as keratin oxidation and conformational transitions, and assess the effect of the conditioner on water mobility and restoration of the hair's internal structure. Consequently, this study provides deeper insights into the hair damage mechanisms and formulation efficacy, thereby offering the scientific foundation for the development of targeted functional hair care products designed for chemically treated or damaged hair.

2. Materials and Methods

2.1. Sample preparation

Human hair samples, including untreated and treated hair (bleached, permed, permed-dyed), were obtained from a hair salon. Melanin (Sigma-Aldrich, USA), ammonium hydroxide solution (Sigma-Aldrich, USA), and hydrogen peroxide (SAMCHUN Chemical, Korea) were used for melanin oxidation experiments. Distilled water (Human Corporation, Korea) was used throughout the experiment. The active ingredients used in the hair conditioner formulations included Polyglyceryl-3 Betainate Malate, Sulfated Castor Oil (active ingredient 1) and Hydrolyzed Soy Protein PG-Propyl Methylsilanediol (active ingredient 2), all by a cosmetic company in Korea. Formulation 1 contained only the treatment base, Formulation 2 included active ingredient 1 added to the base, and Formulation 3 consisted of the base with both active ingredients 1 and 2, formulated as a conditioner. These formulations were applied to bleached hair samples, and the process was repeated 28 times. Following treatment, all hair samples were washed, dried, and chopped for further analysis.

2.2. Instrumentation and characterization

The surface morphology of hair was analyzed using scanning electron microscope (SEM, Hitachi S4800, Japan). Fourier-transform infrared (FT-IR) spectra were acquired by FT-IR spectrometer (Perkin Elmer, USA). Fluorescence images were acquired with optical microscope (Nikon Eclipse Ti2-U, USA). Fluorescence intensity was measured using fluorescence spectrometer (Scinco FluoroMate FS-2, Korea). Solid-state NMR spectroscopy, including ^{13}C CP/MAS and ^{1}H $T_{1\rho}$ relaxation time, were performed using Bruker NMR spectrometer equipped with a 4 mm magic-angle spinning probe (Bruker Biospin, Billerica, MA, USA). Hair samples were chopped and packed into a 4 mm ZrO_2 rotor, which was then sealed with a cap and loaded into the solid-state NMR probe. High-resolution MAS NMR experiments were conducted on NMR spectrometer using HR-MAS probe. For bleached hair and hair treated with formulations, the samples were finely cut and placed into a Kel-F insert, and D_2O (Sigma-Aldrich, USA) was added to the insert to enhance signal detection. The insert was then closed with disposable plug, inserted into the rotor, and loaded into the HR-MAS probe.

3. Results

The morphological differences between untreated and chemically treated hair samples were examined using SEM. As shown in Figure 1, untreated hair has a smooth surface with compact, regularly arranged cuticle layers. In contrast, treated samples–including those subjected to bleaching, perming, combined perming and dyeing–exhibited significant surface damage with

torn and irregularly distributed cuticles. Severely bleached hair showed almost complete loss of the cuticle layer, exposing the internal structure.

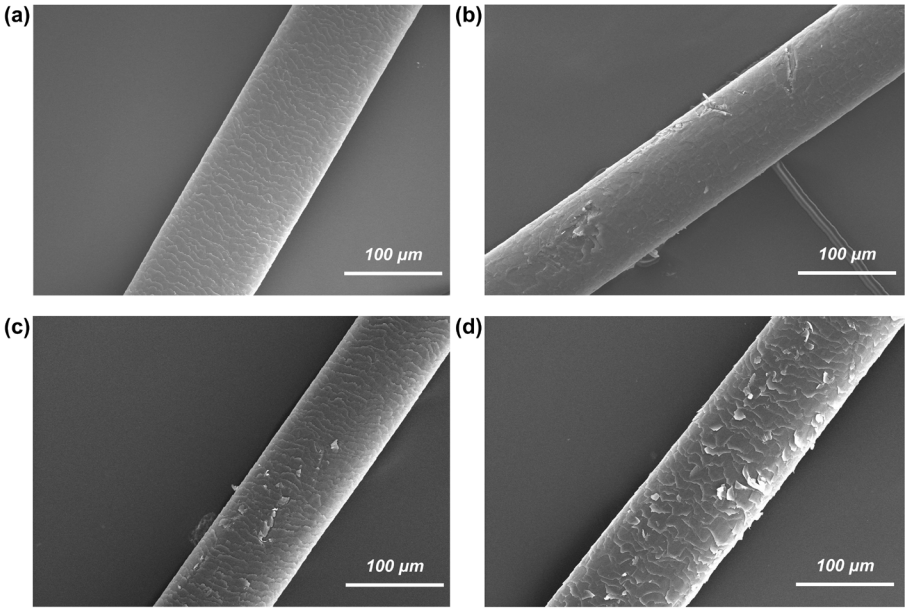

Figure 1. SEM images of the (a) untreated hair and treated hair samples: (b) bleaching, (c) perming, and (d) perming–dyeing.

FT-IR was performed to evaluate chemical alterations in the hair structure after treatment (Figure 2). All samples displayed characteristic absorption bands of keratin, including N–H stretching (3284 cm^{-1}), C-H stretching of CH_2 and CH_3 in aliphatic groups (3000–2800 cm^{-1}), and amide I, II, and III (1637, 1528, and 1231 cm^{-1}, respectively). Notably, treated hair samples exhibited stronger absorption at 1042 cm^{-1}, corresponding to the S=O stretching of cysteic acid due to oxidative cleavage of disulfide bonds.

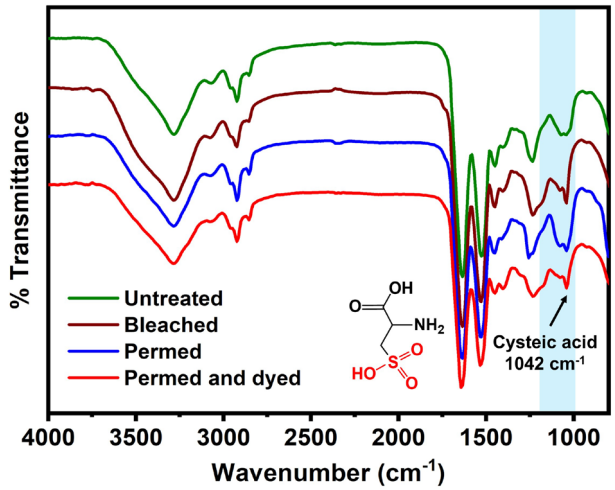

Figure 2. FT-IR spectra of the untreated and treated hair samples and oxidation product of disulfide bonds in keratin structure.

Fluorescence spectroscopic analysis was conducted to investigate melanin oxidation in hair induced by chemical treatments. In our study, synthetic melanin was treated with different concentrations of hydrogen peroxide, a common oxidizing agent in hair treatment products, to simulate oxidative stress. Fluorescence measurements of melanin oxidized by H_2O_2 revealed

new excitation/emission peaks at 470/540 nm (Figure 3a). To visualize these changes at the cellular level, fluorescence microscopy was formed on hair samples using DAPI, GFP, and TRITC filters. Untreated hair showed minimal fluorescence signals due to intrinsic autofluorescence, whereas all treated hair samples exhibited significantly stronger signals in all channels (Figure 3b). Repeated bleaching led to a further increase in signal intensity, indicating cumulative oxidative damage. These findings suggest that fluorescence imaging may serve as a potential marker for melanin oxidation.

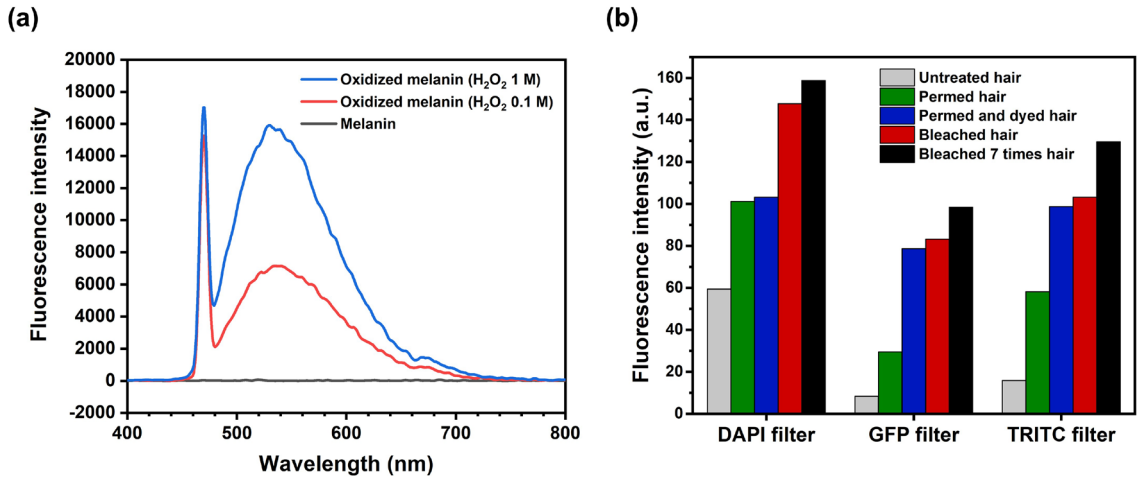

Figure 3. (a) Fluorescence spectra of the melanin samples before and after the oxidation experience with hydrogen peroxide (H_2O_2) reagent, (b) comparison of fluorescence intensities in different filters between each hair sample.

To further explore structural changes of hair, we analyzed the solid-state ^{13}C CP/MAS NMR spectra of untreated and chemically treated hair samples (Figure 4) showed characteristic region. Overlapping signals were deconvoluted and analyzed excluding sideband. In the carbonyl region (165–190 ppm), peaks at approximately 176 ppm and 172 ppm were attributed to α-helix and β-sheet/random coil conformations, respectively. Based on the integration of each carbonyl peak and the total integration (Table 1), the results indicated a decrease in the percentage of α-helix and an increase in the relative area of β-sheet and random coil structures in the treated hair samples compared to untreated hair. Among the chemically processed samples, the combination of perming and coloring led to the most pronounced conformational alterations. These structural modifications became more pronounced in bleached hair, where the α-helix to β-sheet transition was most evident, indicating substantial cumulative damage. In the α-carbon region (46–80 ppm), treated hair show increased intensity at 56 and 49 ppm due to the β-sheet/random coil structure. In contrast, the signal associated with α-helix (58–65 ppm) decreased. The reduction of the 40 ppm peak assigned to β-carbon cross-linked cysteine and leucine is consistent with FT-IR results and further supports disulfide bond breakdown during treatment.

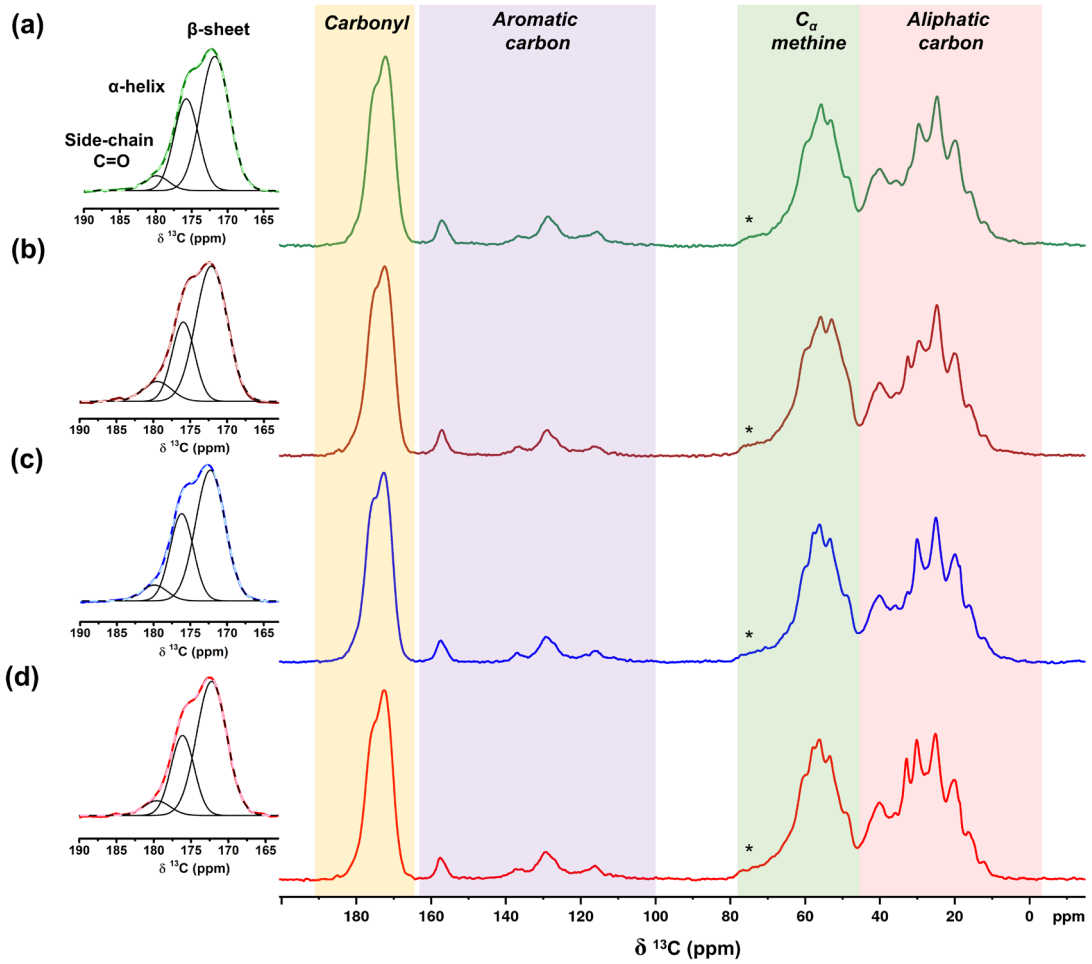

Figure 4. ^{13}C CP/MAS spectra of (a) untreated, (b) bleached, (c) permed, and (d) permed–dyed hair samples. The insets show deconvoluted peaks of carbonyl of each sample.

Table 1. Deconvoluted result of the carbonyl region in the NMR spectrum

v(F1) [ppm]	Untreated	Bleached	Permed	Permed and dyed
Side chain (180 ppm)	5.58	8.71	6.50	6.21
α-helix (176 ppm)	34.47	27.20	32.38	29.51
β-sheet + random coils (172 ppm)	59.95	64.09	61.12	64.25

The structural variations in keratin between different hair samples were investigated by solid-state ^{13}C CP/NMR spectroscopy. To estimate molecular regularity, we measure the proton T_1 relaxation time in the rotating frame (^1H $T_{1\rho}$) at selected carbon position. Treated samples generally had lower $T_{1\rho}$ times at carbonyl (172 ppm), α-carbon at 56 and 53 ppm, and aliphatic carbon at 40 ppm, indicating increased molecular mobility and reduced structural order (Figure 5). These results suggest a transition toward a more disordered (amorphous) keratin conformation.

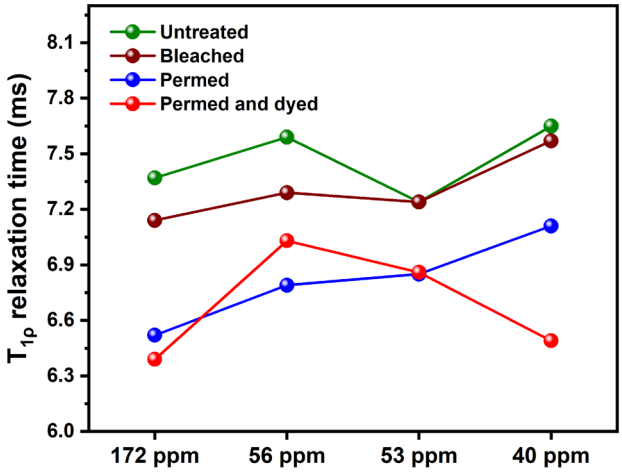

Figure 5. Comparison of ^{1}H $T_{1\rho}$ values of different hair samples.

After applying the conditioners to the damaged hair, HR-MAS NMR analysis was performed to observe the changes in the physical properties of the hair with the different formulations. T_2 relaxation time measurements were conducted on the water NMR signals to assess water mobility in bleached and conditioner-treated hair samples (Figure 6). Due to the potential influence of D_2O solvent on free water, the analysis primarily focused on the bound water compartment, which is critical for evaluating hair elasticity and water retention capacity. As shown in Table 2, the bleached hair had the longest T_2 value, while T_2 times were significantly reduced in hair treated with the formulations added active substances. Among these, formulation 3-treated hair showed the shortest T_2 relaxation time and the highest proportion of bound water, suggesting notable differences in water dynamics induced by conditioner.

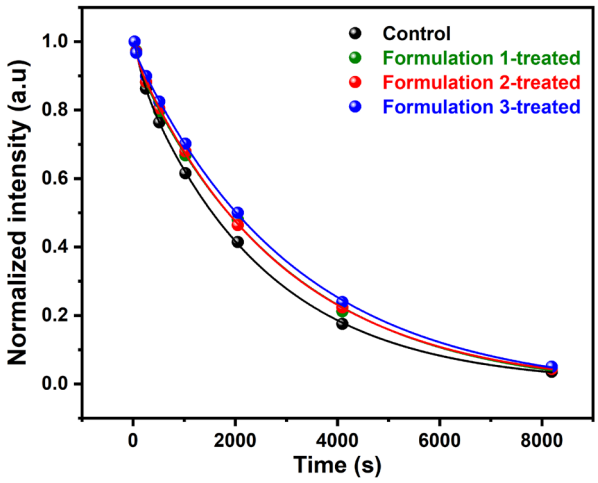

Figure 6. T_2 relaxation time fitting graphs for water signals in control (bleached), F1-treated hair, F2-treated hair, and F3-treated hair.

Table 2. Deconvoluted result of the carbonyl region in the NMR spectrum

Sample	Control	F1-treated	F2-treated	F3-treated
Bound water T_2 (ms)	311.6	191.4	115.4	46.7

A_{bound} (%)	8.9	7.2	7.4	10.7

4. Discussion

The SEM results (Figure 1) indicate that chemical treatments degrade the cuticle layer of hair, leading to increased roughness and potential exposure of the cortex. Such damage undermines the hair's moisture retention and its resilience to external stress. The intensified FT-IR band at 1042 cm^{-1}, corresponds to S=O stretching vibrations of cysteic acid, indicating oxidative conversion of cysteine residues (Figure 2). This transformation is associated with the cleavage of disulfide bonds, which plays a critical role in the mechanical stability of keratin. As more disulfide linkages are broken, the structural integrity of the hair weakens, making it more vulnerable to mechanical and environmental stress. The observed increase in fluorescence intensity (Figure 3) after H_2O_2 treatment implies that melanin undergoes oxidation, amplifying its fluorescence yield. Among the treatment types, bleaching, especially repeated bleaching, caused the most severe oxidation, as evidenced by the strong fluorescence signal. These results validate the use of fluorescence microscopy as a tool to detect and assess the extent of chemical-induced melanin oxidation. In parallel, solid-state ^{13}C NMR analysis (Figure 4) revealed that chemical treatments induce a conformational transition in hair keratin. The reduction in α-helix content and a subsequent increase in β-sheet and random coil indicate disruption of the protein's secondary structure. Since α-helix is stabilized by intramolecular hydrogen bonding and disulfide linkages, the changes demonstrate that chemical agents in the treatment products compromise these stabilizing interactions. This structural transformation can reduce the stiffness and tensile strength of hair while increasing its flexibility and susceptibility to damage. Complementary to the conformational insights from solid-state Additionally, ^{1}H $T_{1\rho}$ relaxation time measurements (Figure 5) provided supporting evidence for increased structural disorder. The overall decrease in $T_{1\rho}$ values across the main chain and side chain regions reflects enhanced molecular mobility and increased amorphous properties. These findings are consistent with the destruction of ordered keratin regions, suggesting weakened structural integrity. Based on the collective findings from these complementary analytical techniques, it is evident that conditioner formulations–particularly those containing active ingredients–can mitigate the structural damage induced by chemical treatments. The reduction in T_2 relaxation time observed in the formulation-treated hair samples indicates a decrease in water mobility within the hair matrix (Figure 6). This result suggests that the treatment may contribute to the formation of more compact hair barrier by improving the internal structure and enhancing the hair's ability to conserve moisture. The improvements in water retention and hair elasticity observed in the NMR analysis are thus closely associated with the restoration of keratin organization and the stabilization of the cuticle structure. This emphasizes the important role of formulation design in developing effective strategies for the protection and repair of chemically damaged hair.

5. Conclusion

In this study, the properties of various hair types subjected to representative cosmetic treatments were investigated using integrative analytical approaches with NMR spectroscopy, providing valuable insights into hair structure and formulation performance. Morphological damage to hair was assessed using SEM, and FT-IR spectroscopy was employed to examine changes in α-keratin structure by analyzing functional group variations. In the treated hair samples, an increase in the intensities of cysteic and its intermediate oxidation products were observed, resulting from the oxidation of cysteine residues in disulfide bonds connecting keratin molecules. The extent of oxidation caused by each treatment was further evaluated via

fluorescence microscopy with melanin pigment as an indicator. All treated hair samples showed higher fluorescence intensities, most prominently in the bleached samples. In addition to FT-IR, solid-state ^{13}C NMR analysis revealed differences in internal structure and molecular regularity between untreated and treated hair samples. $T_{1\rho}$ relaxation time measurements indicated a slight reduction in almost all regions of the treated hair, indicating a decrease in structural integrity after cosmetic treatments. To address this damage, the effectiveness of conditioners was evaluated using HR-MAS NMR and this study demonstrated that formulations containing active ingredients play an important role in hair recovery. Specifically, these formulations significantly affected water mobility within the hair, indicating potential benefits in strengthening the hair barrier and improving water retention. These findings offer a foundation for developing effective hair care solutions tailored to chemically damaged hair, ultimately contributing to progress in the cosmetics industry.

Reference

[1] Csuka, D. A.; Csuka, E. A.; Juhász, M. L. W.; Sharma, A. N.; Mesinkovska, N. A. A systematic review on the lipid composition of human hair. *International journal of dermatology* **2023**, *62* (3), 404.

[2] Boulos, R. A.; Eroglu, E.; Chen, X.; Edwards, B. R.; Toster, J.; Raston, C. L.; Scaffidi, A. Unravelling the structure and function of human hair. *Green Chemistry* **2013**, *15* (5), 1268.

[3] Essendoubi, M.; Meunier, M.; Scandolera, A.; Gobinet, C.; Manfait, M.; Lambert, C.; Auriol, D.; Reynaud, R.; Piot, O. Conformation changes in human hair keratin observed using confocal Raman spectroscopy after active ingredient application. *International Journal of Cosmetic Science* **2019**, *41* (3), 203-212.

[4] Chilakamarry, C. R.; Mahmood, S.; Saffe, S. N. B. M.; Arifin, M. A. B.; Gupta, A.; Sikkandar, M. Y.; Begum, S. S.; Narasaiah, B. Extraction and application of keratin from natural resources: a review. *3 Biotech* **2021**, *11* (5).

[5] Cruz, C. F.; Martins, M.; Egipto, J.; Ribeiro, A.; Cavaco-Paulo, A.; Osório, H. Changing the shape of hair with keratin peptides. *RSC Advances* **2017**, *7* (81), 51581.

[6] Claudia, B.; Naneki, C. M.; Karthikeyan, G.; Xuhao, Z.; Valeria, C.; Marco, M.; Nathan, C. G. Mimicking Natural Human Hair Pigmentation with Synthetic Melanin. *ACS Central Science* **2020**, *6* (7), 1179-1188.

[7] Roldan-Kalil, J.; Zueva, L.; Alves, J.; Sanabria, P.; Inyushin, M.; Tsytsarev, V. Amount of Melanin Granules in Human Hair Defines the Absorption and Conversion to Heat of Light Energy in the Visible Spectrum. *Photochemistry and Photobiology* **2023**, *99* (4), 1092.

[8] Nosanchuk, J. D.; Casadevall, A. Impact of melanin on microbial virulence and clinical resistance to antimicrobial compounds. *ANTIMICROBIAL AGENTS AND CHEMOTHERAPY* **2006**, *50* (11), 3519-3528.

[9] França-Stefoni, S. A.; Dario, M. F.; Sá-Dias, T. C.; Bedin, V.; Almeida, A. J.; Baby, A. R.; Velasco, M. V. R. Protein loss in human hair from combination straightening and coloring treatments. *Journal of Cosmetic Dermatology* **2015**, *14* (3), 204-208.

[10] Grosvenor, A. J.; Deb-Choudhury, S.; Middlewood, P. G.; Thomas, A.; Lee, E.; Vernon, J. A.; Woods, J. L.; Clerens, S.; Taylor, C.; Bell, F. I. The physical and chemical disruption of human hair after bleaching – studies by transmission electron microscopy and redox proteomics. *International Journal of Cosmetic Science* **2018**, *40* (6), 536.

[11] Di Foggia, M.; Taddei, P.; Boga, C.; Nocentini, B.; Micheletti, G. Interactions between Damaged Hair Keratin and Juglone as a Possible Restoring Agent: A Vibrational and Scanning Electron Microscopy Study. *Molecules* **2024**, *29* (2), 320-339.

[12] Kuzuhara, A. Analysis of structural changes in bleached keratin fibers (black and white human hair) using Raman spectroscopy. *Biopolymers* **2006**, *81* (6), 506.

[13] Astbury, W. T.; Street, A. X-Ray Studies of the Structure of Hair, Wool, and Related Fibres. I. General. *Philosophical Transactions of the Royal Society of London. Series A, Containing Papers of a Mathematical or Physical Character* **1932**, *230*, 75-101.

[14] Contreras, F.; Ermolenkov, A.; Kurouski, D. Infrared analysis of hair dyeing and bleaching history. *Analytical Methods* **2020**, *12* (29), 3741.

[15] Nishikawa, N.; Horiguchi, Y.; Asakura, T.; Ando, I. Carbon-13 solid-state n.m.r. study of 13C-enriched human hair keratin. *Polymer* **1999**, *40* (8), 2139-2144.